

# Wavelength synergistic effects in continuous flow-through water disinfection systems

Adithya Pai Uppinakudru<sup>a,b</sup>, Miguel Martín-Sómer<sup>a</sup>, Ken Reynolds<sup>b</sup>, Simon Stanley<sup>b</sup>, Luis Fernando Bautista<sup>a</sup>, Cristina Pablos<sup>a,\*</sup>, Javier Marugán<sup>a</sup>

<sup>a</sup> Department of Chemical and Environmental Technology, ESCET, Universidad Rey Juan Carlos, C/ Tulipán S/n, 28933, Mostoles, Madrid, Spain

<sup>b</sup> ProPhotonix IRL LTD, 3020 Euro Business Park, Little Island, Cork, T45×211, Ireland

## ARTICLE INFO

### Keywords:

*E. coli*  
Disinfection  
Kinetic constant  
Synergy  
Ultraviolet light  
Wastewater

## ABSTRACT

The past decade's development of UV LEDs has fueled significant research in water disinfection, with widespread debate surrounding the potential synergies of multiple UV wavelengths. This study analyses the use of three UV sources (265, 275, and 310 nm) on the inactivation of *Escherichia coli* bacteria in two water matrices. At maximum intensity in wastewater, individual inactivation experiments in a single pass set-up (Flow rate = 2 L min<sup>-1</sup>, Residence time = 0.75 s) confirmed the 265 nm light source to be the most effective (2.2 ± 0.2 log units), while the 310 nm led to the lowest inactivation rate (0.0003 ± 7.03 × 10<sup>-5</sup> log units). When a combination of the three wavelengths was used, an average log reduction of 4.4 ± 0.2 was observed in wastewater. For combinations of 265 and 275 nm, the average log reductions were similar to the sum of individual log reductions. For combinations involving the use of 310 nm, a potential synergistic effect was investigated by the use of robust statistical analysis techniques. It is concluded that combinations of 310 nm with 265 nm or 275 nm devices, in sequential and simultaneous mode, present a significant synergy at both intensities due to the emission spectra of the selected LEDs, ensuring the possibility of two inactivation mechanisms. Finally, the electrical energy per order of inactivation found the three-wavelength combination to be the most energy efficient (0.39 ± 0.05, 0.36 ± 0.01 kWh m<sup>-3</sup>, at 50% and 100% dose, respectively, in wastewater) among the synergistic combinations.

## 1. Introduction

Wastewater is any water that has been used and discarded by humans, typically as a result of domestic, commercial or industrial activities (UN Water, 2023). This discarded water may contain a wide range of impurities, including human and animal waste, food waste, and other harmful pollutants (UNICEF, 2019). Wastewater disinfection is important for several reasons, including, but not limited to, protecting public health and the environment (USEPA, 2023).

Disinfection is a requirement for wastewater reuse purposes as per the updated regulation 2020/741 of the European Parliament (EU) and of the council on minimum requirements for water reuse (Regulation (EU) 2020/741, 2022). Multiple technologies have successfully disinfected wastewater and evaluated potential transformation products (Tchobanoglous and Burton, 1990; Mecha et al., 2017; Rodríguez-Chueca et al., 2019). However, studies on the use of multiple wavelengths for effective disinfection of wastewater have been limited.

Ultraviolet (UV-C) light is known for its power to inactivate and kill bacteria, viruses, and parasites that could harm humans. Since the early 2000's, a new technology of light emitting diodes (LEDs), emitting light in UV-C region of the spectrum, holds promise to replace mercury lamps in wastewater treatment. Wastewater is a cause of serious concern for governments and communities across the world. While there has been significant progress in disinfection research using other techniques such as chlorination, ozonation, and membrane filtration, the number of studies on the use of UV-C LEDs to treat wastewater has been seen to be limited (Rout et al., 2021; Collivignarelli et al., 2021; Song et al., 2016; Kang and Kang, 2019; Ashok and Khedikar, 2016).

The existence of potential synergy between multiple wavelengths in disinfection has been widely debated across the literature. Synergy occurs when the combination of multiple wavelengths produces an effect greater than the sum of their separate effects (Beck et al., 2017). Some researchers have found no synergistic effect (Hull and Linden, 2018; Nyangaresi et al., 2019; Woo et al., 2019), while others have reported a

\* Corresponding author.

E-mail address: [cristina.pablos@urjc.es](mailto:cristina.pablos@urjc.es) (C. Pablos).

significant synergistic effect (Green et al., 2018; Li et al., 2017; Naka-hashi et al., 2014). For instance, Beck et al. (2017) conducted experiments using UVinaire® dual wavelength UV-C LEDs unit (Aquisense) to study potential synergy between 260 nm and 280 nm UV-C LEDs and concluded that synergy was not possible due to the 2<sup>nd</sup> law of

photochemistry (Beck et al., 2017). However, although the argument stated is true, it is important to note that the inactivation mechanisms of the two wavelengths used on the microorganisms, are similar, hence any combined effect would merely be the result of the sum of individual wavelength effects (Beck et al., 2017). Contrary to the aforementioned

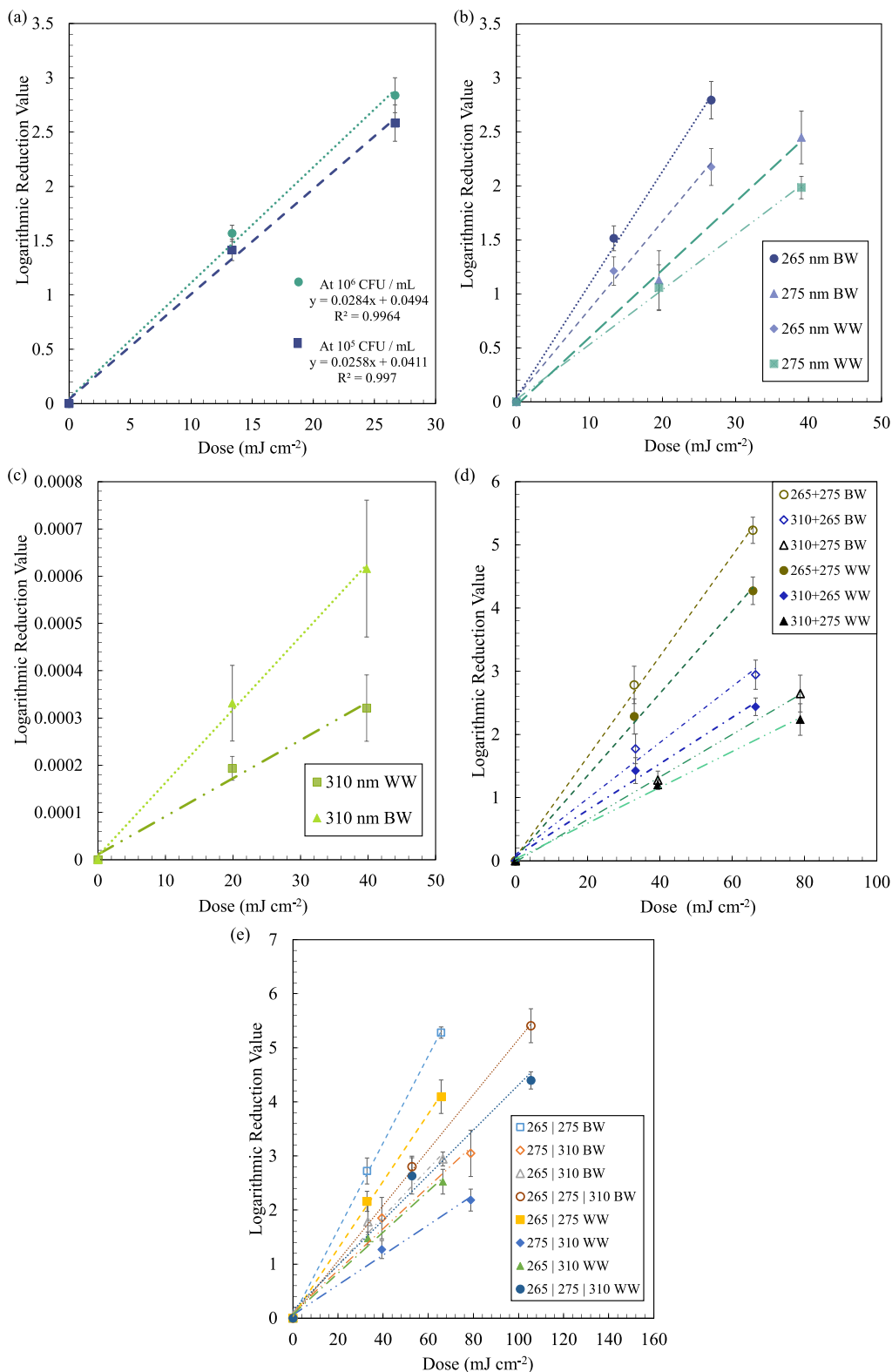


**Fig. 1.** (a) Comparison between inactivation rates for two bacterial concentrations within a single pass reactor for FX-1 265, LRV vs UV dose, in both matrices, for (b) FX-1 265, 275 and (c) FX-1 310, (d) SE mode, and (e) SI mode (Legend - BW = Buffered Water and WW = Wastewater).

research, Green et al. (2018) concluded that there was synergistic inactivation of three common foodborne pathogens when illuminating the water surface with a combination of 259 nm and 289 nm UV light (Pearl Beam™ collimated beam unit (Aquisense)), due to possible alternative inactivation mechanism at 289 nm leading to enhanced disinfection. This has led to questions being raised on other possible parameters like emission spectrum, type of device, and contribution of each wavelength, when in combination, that could play a key role in comprehensively understanding synergy between wavelengths (Green et al., 2018; Song et al., 2016; Matafonova and Batoev, 2022).

In all the studies on synergy so far, authors have had little to no control over the light sources used. The need for faster and more effective inactivation processes is of growing need, given the extremities of water safety being discussed worldwide. Synergy of multiple wavelengths could provide a solution to this growing demand and also possibly result in lower energy consumption for higher disinfection rates. This study presents novel and conclusive research on the synergistic interactions among multiple wavelengths of LEDs light in the UV region of the spectrum. It is conducted with a focus on forming a comprehensive understanding of the attributes of the light source, the associated device, and the characteristics of light emission. It attempts to investigate synergy by custom selecting UV-C and UV-B LEDs sources and to study their resulting combination effect on the inactivation of *E. coli* K12 and *wild E. coli* in a buffered and wastewater matrix, respectively. The experimental set-up allows exposure of multiple wavelengths, in various combinations, to a single pass flow reaction. The study verifies any possible synergistic effect by the use of robust statistical analysis tools and attempts to correlate the observed effect with the inactivation mechanisms of the employed wavelength ranges. Finally, the study evaluates the electrical energy per unit order of inactivation to conclude if the combination of wavelengths increased or decreased the energy efficiency of the overall process.

## 2. Results and Discussions

### 2.1. Kinetic order and effect of dose

For the single pass continuous flow reactor, it was necessary to verify that the reaction follows first-order kinetics with respect to the concentration of bacteria, and a linear dependence with the radiation dose (Bolton and Linden, 2003). For this purpose, two bacterial concentrations ( $10^6$  and  $10^5$  colony forming units per mL (CFU mL<sup>-1</sup>)) were tested at two UV dose levels, the maximum emitted by the device (100%) and half this value (50%) for FX-1 265 device. The experiments were repeated a minimum of 3 times to ensure repeatable and reproducible data were obtained. The plot of logarithmic reduction values (LRV) vs UV dose can be found in Fig. 1 (a). It was seen that a change in the initial concentration of bacteria did not affect the inactivation rate within the reactor. The slopes of the two bacterial concentrations were compared to

verify the similarity and it is clear that the two concentrations behave similarly within the reactor set-up. Further validation of the first-order kinetics was carried out at multiple dose levels using three different irradiation levels (50%, 75% and 100%) and three flow rates (1.5, 1.75 and 2 L min<sup>-1</sup>). With a reduction in flow rate, the residence time increases and consequently the UV dose received, confirming a clear linear effect of the UV dose in the studied range of variables (data not shown). Hence, it has been concluded that the single pass flow reactor experiments follow a first-order kinetics.

### 2.2. UV inactivation by individual wavelengths

To elucidate any possible synergistic effect between multiple wavelengths, it is necessary to completely understand the effect of individual wavelengths on the inactivation. Table 1 lists the actual LRV for individual wavelengths. Fig. 1(b, c) plots the LRV with an increase in UV dose on the matrix. It is worth noting that the FX-1 310 experiments were attempted in a single pass, but the LRV values were negligible. Therefore, the average log reduction per pass for the FX-1 310 was estimated from the recirculation experiments until 1-log reduction (Further details can be found in Section A, Supplementary information (SI)).

All wavelengths show linear behavior with an increase in dose, as shown in Fig. 1(b, c). In both water matrices, FX-1 265 showed the highest LRV over the other two wavelengths. At 100% intensity,  $2.8 \pm 0.2$  and  $2.2 \pm 0.2$  log reductions were achieved in buffered water (BW) and wastewater (WW), respectively. The emission from this device peaks at 269.03 nm, which is relatively well absorbed by the DNA/RNA in *E. coli* (Fig. 2(a)), leading to the formation of thymine dimers and, consequently, distortion of the DNA structure within the microorganism (Hiraku et al., 2007; Bolton and Cotton, 2008). While FX-1 275 (Peak wavelength of 277.74 nm) operates with the same inactivation mechanism as that of FX-1 265, the absorption of this wavelength by *E. coli* K12 is lower than that of FX-1 265 LEDs (See Fig. 2(a)) (Bolton and Cotton, 2008) and therefore is second best when comparing the LRVs (at 100% intensity, reductions of  $2.5 \pm 0.3$  and  $1.9 \pm 0.1$  log units in BW and WW respectively). The average LRV of the FX-1 310 is extremely low, almost insignificant in a single pass reactor (at 100% intensity, reductions of  $0.00062 \pm 0.00015$  and  $0.0003 \pm 7.03 \times 10^{-5}$  log units, in BW and WW respectively) as the emission of this device is predominantly in the UV-B, UV-A region of the spectrum (~90% of the total spectral emission). This wavelength range is less energetic than the UV-C range in causing damage and is known to cause indirect damage by generation of reactive oxygen species (ROS) (Hiraku et al., 2007), repair inhibition (Li et al., 2017) and cell membrane damage (Pizzaro, 1995).

Comparing the two matrices, LRV at similar doses showed that *wild E. coli* may be more UV resistant compared to *E. coli* K12. It is worth noting here that, although the bacteria were spiked to the effluent, there exist other microorganisms that compete with the *wild E. coli* for the

**Table 1**  
Observed actual LRV for UV sources and combinations.

UV Source / Combination	Buffered Water Matrix				Wastewater Matrix			
	Average LRV (50% Dose)	Average LRV (100% Dose)	R <sup>2</sup>	k <sub>d</sub> (cm <sup>2</sup> mJ <sup>-1</sup> )	Average LRV (50% Dose)	Average LRV (100% Dose)	R <sup>2</sup>	k <sub>d</sub> (cm <sup>2</sup> mJ <sup>-1</sup> )
FX-1 265	1.52 ± 0.12	2.8 ± 0.2	0.997	0.1047	1.2 ± 0.1	2.2 ± 0.2	0.996	0.0815
FX-1 275	1.13 ± 0.27	2.5 ± 0.3	0.997	0.0627	1.1 ± 0.2	1.9 ± 0.1	0.999	0.0508
FX-1 310	0.0003 ± 0.00008	0.00062 ± 0.00015	0.998	$2 \times 10^{-5}$	0.0002 ± 2.52 × 10 <sup>-5</sup>	0.0003 ± 7.03 × 10 <sup>-5</sup>	0.986	$8 \times 10^{-6}$
265 + 275	2.8 ± 0.3	5.2 ± 0.2	0.998	0.079	2.3 ± 0.3	4.3 ± 0.2	0.998	0.0650
310 + 265	1.8 ± 0.2	3.0 ± 0.2	0.986	0.044	1.4 ± 0.2	2.4 ± 0.1	0.990	0.0367
310 + 275	1.3 ± 0.2	2.6 ± 0.3	0.999	0.033	1.20 ± 0.07	2.2 ± 0.3	0.998	0.0284
265 275	2.7 ± 0.2	5.3 ± 0.1	0.999	0.080	2.2 ± 0.2	4.1 ± 0.3	0.999	0.0623
275 310	1.8 ± 0.3	2.9 ± 0.1	0.984	0.038	1.3 ± 0.2	2.2 ± 0.2	0.991	0.0277
265 310	1.8 ± 0.4	3.0 ± 0.4	0.985	0.044	1.5 ± 0.1	2.5 ± 0.2	0.990	0.0380
265 275 310	2.8 ± 0.2	5.4 ± 0.3	0.999	0.051	2.6 ± 0.4	4.4 ± 0.2	0.987	0.0417

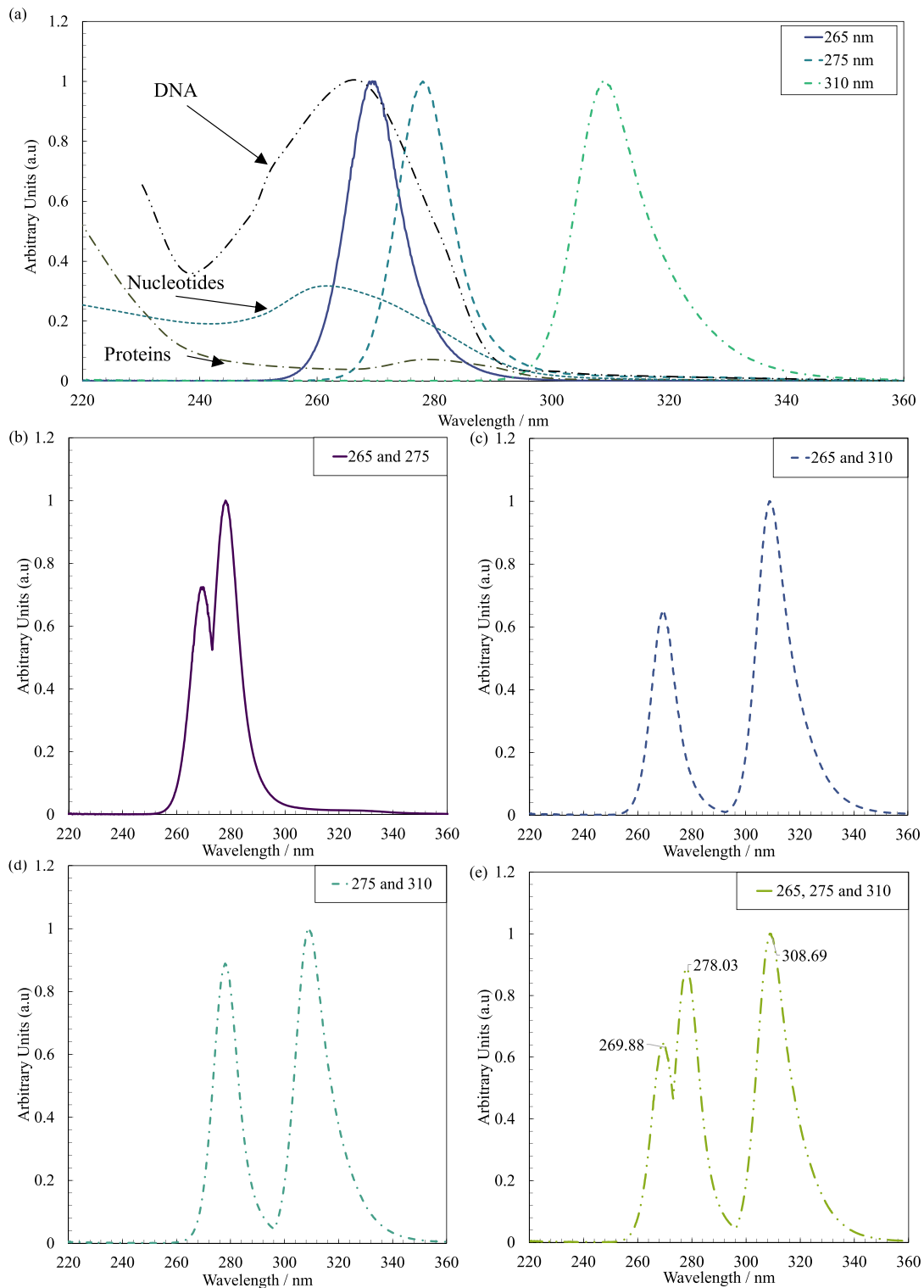


**Fig. 2.** (a) Individual wavelength spectra of the light sources relative to their respective peaks alongside absorption spectra for DNA, proteins, and nucleotides extracted from Bolton and Cotton, 2008; Payne and Sancar, 1990, combined emission spectrum relative to maximum intensity measured for (b) 265/275, (c) 265/310, (d) 275/310, and (e) 265/275/310 combinations.

light and could affect the inactivation rate together with the effect of the chemical composition of WW. Chemicals such as ions and organic matter may interfere, hindering the inactivation process.

### 2.3. UV inactivation by combination of wavelengths

Inactivation experiments were conducted for all possible combinations shown in Fig. 3(f-h), for a minimum of 4 replicates on separate days, to ensure that the data obtained is repeatable and reproducible. Actual LRV and  $k_d$  values (kinetic constants based on UV dose) for each

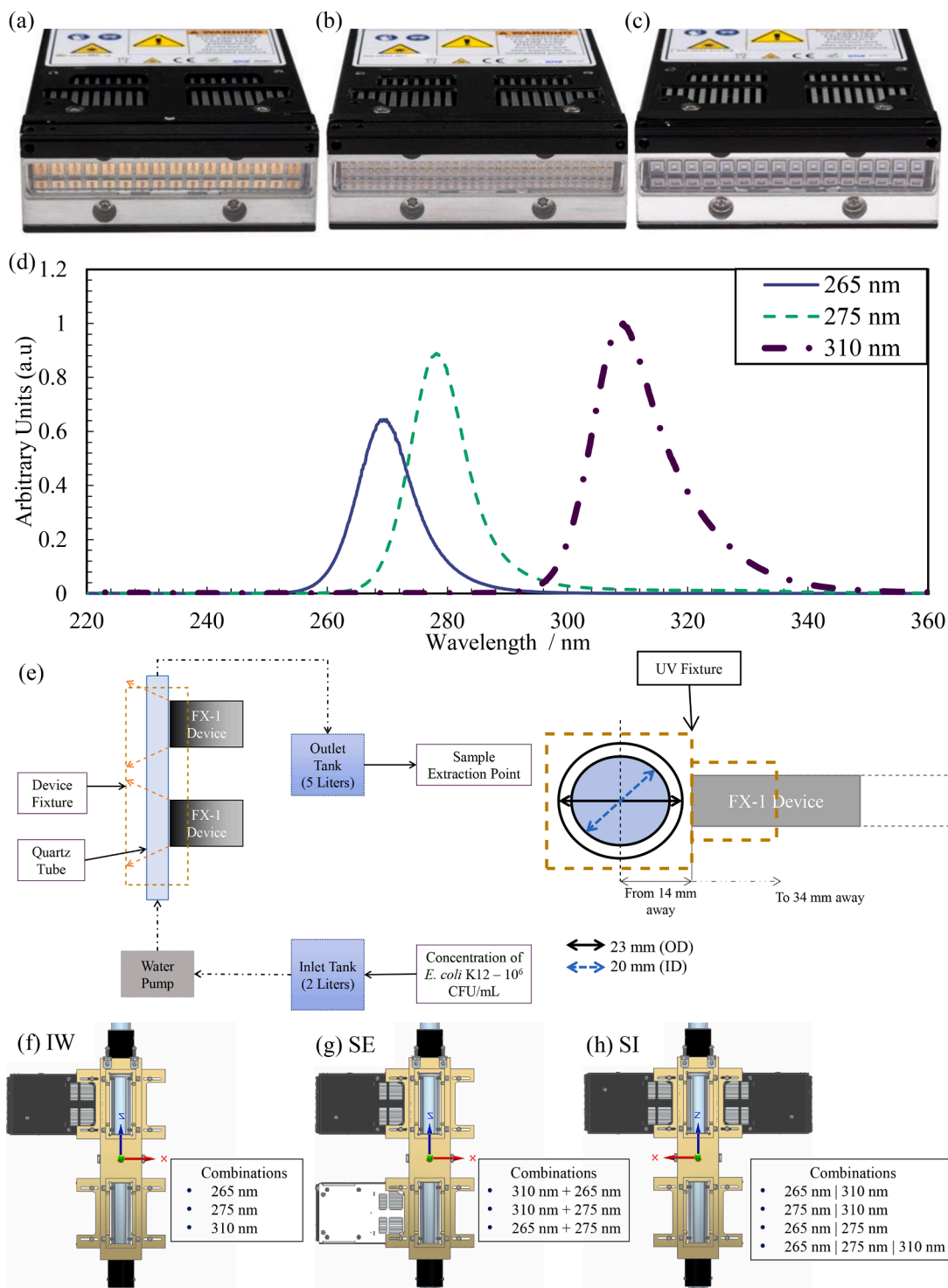


**Fig. 3.** - COBRA Clean FX-1 (a) 265 nm LEDs source (Klaran), (b) 275 nm LEDs source (Luminus), and (c) 310 nm LEDs source (EpiGap), (d) Spectra relative to the measured maximum peak at 309.52 nm, (e) schematic representation of the experimental set-up and distance between centre of the tube to source window and possible combinations on UV fixture - (f) individual wavelengths (IW), (g) sequential mode (SE), and (h) simultaneous mode (SI).

combination are listed in Table 1. For data on the first-order kinetic constant ( $k_c$  in  $s^{-1}$ ), see Section B(SI).

**2.3.1. Sequential mode (SE)**

Sequential mode involves the exposure of the water to two devices, one after the other. Fig. 1(d) plots the observed LRV against the UV dose acting on both water matrices. It is important to note that the order of exposure in the legend is the first wavelength followed by the other i.e.,

310 + 265 corresponds to first exposure to FX-1 310 and then FX-1 265. The other order of irradiation has also been attempted and the effect of the order of irradiation has been discussed in Section C(SI). The order of inactivation rates for the highest inactivation, at  $\sim 60 \text{ mJ cm}^{-2}$ , is  $LRV(265 + 275) > LRV(310 + 265) > LRV(310 + 275)$ . As expected, considering the direct mechanism of DNA damage may be occurring at both wavelengths, the combination of FX-1 265 and 275 presented the maximum inactivation in viable bacterial concentration at similar dose

levels compared to the other combinations in this mode. In contrast, the order of irradiation of the devices presented a significant effect for the other combinations involving FX-1 310 with 265 or 275 nm devices. The radiation of FX-1 310, first, followed by the FX-1 265 or 275 was found to be more effective than vice versa (Section C, SI).

2.3.2. Simultaneous mode (SI)

In the simultaneous mode of operation (Fig. 3(h)), all the wavelengths under study act at the same instant of time and the same point. In SI mode of irradiation (Fig. 1(e)), the order of inactivation, for both matrices was as expected i.e., at ~60 mJ cm<sup>-2</sup>, LRV (265|275) ~ LRV (265|275|310) > LRV (265|310) > LRV (275|310). Similar to the observations in SE mode, the combination of FX-1 265 and 275 resulted in the highest inactivation at ~60 mJ cm<sup>-2</sup> compared to the other combinations tested. It can also be seen that the combination of FX-1 310 with FX-1 275 resulted in lower inactivation compared to its combination with FX-1 265. Interestingly, the combination of three wavelengths resulted in a similar inactivation at 100% UV dose, of all three devices, when compared to the combination of 265|275. In contrast, this 3-wavelength combination used nearly 1.6 times higher dose than the 265|275 combination.

An additional mode of irradiation was also tested in this work, namely the sequential plus simultaneous mode of irradiation (SS). The SS mode of irradiation was seen to be similar to the SI mode of irradiation of three wavelengths (Fig. 1 (e), circle markers), confirmed by statistical analysis, and hence has not been discussed in this article. Details of the comparison and LRV can be found in Section D(SI).

2.4. Synergy of inactivation

Synergy of inactivation values have been calculated using the definition discussed in Section 3.7 and listed in Table 2. This analysis has also been conducted in terms of kinetic constants (k<sub>c</sub>) and data can be found in Section B(SI). At first glance, it can be confirmed that, for all combinations tested, no antagonism can be seen in the process i.e., the use of multiple wavelengths did not reduce the inactivation rate. In all cases, at least a summation effect of the wavelengths has been observed (Oguma et al., 2013).

In all combinations studied, the Synergy values were close to or greater than 1. However, most of the propagated errors can be seen to overlap with 1 and to conclude the existence of a synergistic effect, this value must be significantly greater than 1 (Beck et al., 2017; Nyangaresi et al., 2019; Koivunen and Heinonen-Tanski, 2005). t-Student analysis was first employed to check for the statistical significance of the difference between theoretical and actual LRVs obtained in this study. The technique has been detailed in Section 3.8.2. Table 2 lists the observations (in italics under SO column) for each combination based on the argument discussed. Given the closeness between the observation of “significant (S)” and “not significant (NS)” effect for the combinations, it was necessary to correlate results from ANOVA to substantiate any observations of synergistic effect. The obtained p-values have been listed in Table 2 (numbers in SO column). Detailed results from this analysis for all combinations can be found in Section E, SI. The p-values with \* in

Table 2 are cases in which there is a significant difference between the sum of LRVs from individual wavelengths and the LRV in combination. It is worth noting that the 0.0000 value means that the theoretical and actual values are statistically different, with a significant level above 99.99%, as the p-value is lower than 10<sup>-4</sup>.

From Table 2, it was seen that irrespective of the mode of irradiation, the combinations of FX-1 265 nm and 275 nm showed no synergistic effect in either water matrices. In combinations of FX-1 310 nm with FX-1 265 nm, t-Student analysis showed “potential” synergy between the wavelengths, and this was confirmed with the ANOVA results. In this combination, it was seen that SI mode of irradiation in buffered water matrix, at 50% dose each, showed no significant synergistic effect whereas at 100% dose each, there is a potential synergistic effect. Upon closer analysis of the ANOVA results, the p-value for 265|310 combination is just above the 95% CI chosen and it is possible that the experimental error is playing a role in this case. If the CI is chosen at a 94% interval, then potential synergistic effect can also be concluded between the two wavelengths. However, this has not been done to ensure consistency between all the analyses conducted. On the other hand, in the wastewater matrix, this combination showed a significant synergistic effect with 99.99% confidence.

For combinations of FX-1 310 nm with FX-1 275 nm, both modes of irradiation (SE and SI), presented a significant synergistic effect in both matrices. Comparing the two combinations i.e., 265/310 and 275/310 combinations, Table 2, is seen that the synergistic effect is more prominent in the 275/310 nm SI combinations. This could be because in this combination, both wavelengths contribute equally to the total UV dose. In the case of three wavelength combinations, the t-Student analysis found that there was no significant difference. However, from ANOVA we found that there exists a significant difference between the two variables with up to 99.99% confidence.

2.4.1. Synergistic damage mechanism

Among the three wavelengths selected, FX-1 310 emits the maximum intensity (52.9 ± 9.9 mW cm<sup>-2</sup>). Using the measured spectrum, peak wavelength, the full width at half maximum (FWHM) of the LEDs and

Table 3 Device emission characteristics at 100% intensity.

UV Source	Peak wavelength (nm)	FWHM (nm)	% SC below FWHM (From 200 nm)	% SC within the FWHM	% SC above FWHM (until 400 nm)
FX-1 265	269.03	12.39	12.8% (< 264 nm)	67.4% (b/n 264 - 277 nm)	19.8% (> 277 nm)
FX-1 275	277.74	10.64	12.1% (< 273 nm)	64.8% (b/n 273 - 283 nm)	23.1% (> 283 nm)
FX-1 310	309.51	13.99	10.8% (< 303 nm)	63.2% (b/n 303 - 317 nm)	26.0% (> 317 nm)

Table 2 Synergy of inactivation values (by LRV) alongside statistical analysis observations (SO) (t-Student Observations (at 95% Confidence Interval (CI)) - p-value (p < 0.05)).

UV Combination	Buffered Water Matrix				Wastewater Matrix			
	Synergy (BW_50%)	SO	Synergy (BW_100%)	SO	Synergy (WW_50%)	SO	Synergy (WW_100%)	SO
265 + 275	1.06 ± 0.13	NS - 0.7871	0.99 ± 0.04	NS - 0.4329	1.01 ± 0.14	NS - 0.5718	1.03 ± 0.06	NS - 0.2235
310 + 265	1.17 ± 0.16	S - 0.0000	1.05 ± 0.09	S - 0.0041*	1.18 ± 0.18	S - 0.0009*	1.1 ± 0.1	S - 0.0000*
310 + 275	1.13 ± 0.19	S - 0.0016*	1.08 ± 0.13	S - 0.0004*	1.14 ± 0.12	S - 0.0016*	1.13 ± 0.13	S - 0.0004*
265 275	1.03 ± 0.11	NS - 0.4107	1.01 ± 0.02	NS - 0.0774	0.95 ± 0.09	NS - 0.3237	0.99 ± 0.08	NS - 0.3042
265 310	1.2 ± 0.2	S - 0.0614	1.05 ± 0.05	S - 0.0000*	1.2 ± 0.1	S - 0.0000*	1.16 ± 0.11	S - 0.0000*
275 310	1.6 ± 0.5	S - 0.0000*	1.2 ± 0.2	S - 0.0000*	1.2 ± 0.2	S - 0.0003*	1.1 ± 0.1	S - 0.0012*
265 275 310	1.06 ± 0.09	NS - 0.0000*	1.03 ± 0.06	NS - 0.0000*	1.2 ± 0.2	NS - 0.0000*	1.06 ± 0.04	NS - 0.0000*

percentage spectral contributions (% SC), before and after the half maximum, have been calculated. Table 3 lists the measured source emission characteristics for each of the chosen UV LEDs. Fig. 2(a) plots the measured spectrum alongside the absorption spectra of DNA, protein and nucleotides, extracted from Bolton and Cotton, 2008 and Payne and Sancar, 1990, to evaluate and understand potential damage mechanisms occurring within the selected microorganisms. Figs. 2(b-e) display overlapping spectra, illustrating all conceivable combinations of the three wavelengths chosen in this investigation. This plots aims to comprehend the behavior of each wavelength when combined with others.

For the 265 and 275 nm LEDs combinations (see Fig. 2(b)), the 275 nm spectrum overlaps 50% width of 265 nm, with negligible emission above 300 nm. The majority of the combined emission falls in the range of 260-285 nm, similar to the studies by Beck et al., 2017 and Woo et al., 2019. In such cases, a single mechanism of inactivation is potentially occurring, i.e., the direct UV absorption by DNA, resulting in the formation of lesions inhibiting the transcription and replication processes in the microorganism (Bolton and Cotton, 2008; Hiraku et al., 2007; Kuball et al., 2017; Rastogi et al., 2010; Cockell and Airo, 2002). Concurrently, in this combination, the value of synergy of inactivation ( $1.01 \pm 0.02$ ,  $0.99 \pm 0.08$  in BW and WW, respectively) can be seen to be an indicator of the sum of individual wavelength inactivation. Thus, explaining why no significant synergistic effect was seen for SE and SI modes of irradiation for these LEDs combination.

In the case of 265/310 and 275/310 combinations, in both SE and SI modes of irradiation, significant synergy was observed (with a minimum of 94% confidence). In such combinations, it was seen that the 310 nm device has the highest spectral width (13.99 nm) and 26% SC above 317 nm. This indicates that there could be a second inactivation mechanism involved along with a direct mode of inactivation (Fig. 2(c, d)). This range of wavelengths (320-400 nm) has been extensively reported to activate both endogenous and exogenous photosensitizers, leading to the oxidation of biomolecules and, ultimately, cellular death (Kumar et al., 2015; Maclean et al., 2008; Tang and Sillanpää, 2015). Also, low doses have been proven to induce many physiological alterations (Eisenstark et al., 1996; Hiraku et al., 2007). Therefore, it can be concluded that two mechanisms of inactivation are in play for 310 nm - 265/275 nm combinations i.e., direct DNA damage (by FX-1 265 or 275) and indirect damage by physiological alterations (by FX-1 310), leading to a synergistic effect.

Similarly, for combinations of three wavelengths (Fig. 2(e)), the two damage mechanisms mentioned earlier occur during the process, resulting in synergistic effects. However, it must be noted that in three wavelength combinations, the contribution of direct mode of inactivation is greater (global result) than the physiological alteration mechanisms, as the number of photons from FX-1 265 nm and 275 nm contributes to about 63% of the total dose received.

## 2.5. Electrical energy consumption ( $E_{EO}$ )

The trade-off between wavelength, inactivation efficacy, and energy consumption of devices is an important consideration when selecting treatment wavelengths. A comparison between the electrical energy consumption per unit order of inactivation (considering electrical consumption of the pump in each condition) for both matrices is presented in Table 4. The FX-1 265 nm, which is the most efficient of the UV sources in bacterial inactivation, showed the lowest energy consumption corresponding to  $0.55 \pm 0.03$  kWh  $m^{-3}$  and  $0.39 \pm 0.02$  kWh  $m^{-3}$ , at 50% and 100% UV dose, respectively in the wastewater matrix. It was seen that the combination of 265 nm and 275 nm devices (in SE and SI mode) presented a highly energy efficient process because of their combined direct DNA inactivation mechanisms. However, no significant synergistic effect was obtained.

In SE mode, the combination of 310 nm followed by 265 nm granted the lowest energy consumption of  $0.58 \pm 0.08$  kWh  $m^{-3}$  and  $0.49 \pm$

**Table 4**

Electrical energy consumption per unit order of inactivation  $E_{EO}$  (kWh  $m^{-3}$ ) for the tested matrices.

UV Source/ Combination	Buffered Water Matrix		Wastewater Matrix	
	50% intensity	100% intensity	50% intensity	100% intensity
FX-1 265	$0.44 \pm 0.04$	$0.30 \pm 0.03$	$0.55 \pm 0.03$	$0.39 \pm 0.02$
FX-1 275	$0.60 \pm 0.20$	$0.40 \pm 0.10$	$0.64 \pm 0.12$	$0.44 \pm 0.03$
FX-1 310	$1953 \pm 190$	$1332 \pm 275$	$3347 \pm 364$	$2558 \pm 486$
265 + 275	$0.31 \pm 0.05$	$0.24 \pm 0.02$	$0.38 \pm 0.04$	$0.30 \pm 0.02$
310 + 265	$0.50 \pm 0.10$	$0.41 \pm 0.06$	$0.58 \pm 0.08$	$0.49 \pm 0.03$
310 + 275	$0.70 \pm 0.10$	$0.46 \pm 0.06$	$0.71 \pm 0.06$	$0.55 \pm 0.08$
265   275	$0.32 \pm 0.02$	$0.24 \pm 0.02$	$0.4 \pm 0.1$	$0.30 \pm 0.03$
265   310	$0.50 \pm 0.10$	$0.41 \pm 0.02$	$0.56 \pm 0.04$	$0.47 \pm 0.06$
275   310	$0.50 \pm 0.10$	$0.41 \pm 0.04$	$0.67 \pm 0.09$	$0.56 \pm 0.06$
265   275   310	$0.37 \pm 0.02$	$0.29 \pm 0.01$	$0.39 \pm 0.05$	$0.36 \pm 0.01$

$0.03$  kWh  $m^{-3}$ , at 50% and 100% UV dose from each device, respectively, which was found to be similar to the FX-1 265 nm irradiating alone. The same was seen for combinations of 310 nm followed by 275 nm compared to individual wavelength  $E_{EO}$ . However, the energy consumption, in combination, was higher than the FX-1 265 nm alone.

In SI mode, it was seen that a three-wavelength combination (265/275/310) conferred the lowest energy consumption process corresponding to  $0.39 \pm 0.05$  kWh  $m^{-3}$  and  $0.36 \pm 0.01$  kWh  $m^{-3}$ , at 50% and 100% UV dose, respectively when compared to the other combinations. This combination was found to be most efficient in terms of inactivation and electrical energy consumption.

When comparing the  $E_{EO}$  values reported to Beck et al., 2017 for reducing *E. coli* using low-pressure UV (LP UV,  $0.0006 \pm 1$ SD kWh  $m^{-3}$  per 2-log reduction) and medium-pressure UV (MP UV,  $0.013 \pm 1$ SD kWh  $m^{-3}$  per 2-log reduction) lamps, it becomes apparent that UV LEDs still consume significantly more electrical power as compared to conventional mercury lamps. Specifically, the LEDs in this study exhibited output power efficiencies of 2.29%, 1.32%, and 2.38% for FX-1 265, 275, and 310, respectively (Table 5). These efficiencies are particularly lower than those of LP/MP UV lamps. While this might seem discouraging, it is worth noting that the landscape for UV LEDs has evolved, particularly with the resurgence of UV LEDs during the recent global pandemic. In recent years, many manufacturers have reported substantially higher output efficiencies for UV LEDs (7% wall plug efficiency, S6060 SMD 265 nm, Bolb), and the UV LED manufacturing market is poised for significant growth in the coming decade suggesting that the limitations of LEDs technology in terms of power consumption are being actively addressed and improved upon (Martín-Sómer et al., 2023). Finally, it is worth noting that the system likely operates under laminar flow regime ( $Re = 2377$ , Section F, SI). Therefore, a more comprehensive fluid dynamic analysis of the system should be conducted to ensure the effective operation of large-scale applications operating under turbulent flow.

## 3. Conclusions

The study presented a novel UV LEDs device, demonstrating its efficacy in wastewater disinfection by carefully selecting three UV region wavelengths. A synergistic effect between multiple wavelengths was observed in this study for both water matrices tested. Due to the spectral emission of the selected devices, two inactivation mechanisms, in ranges of 250-320 nm (direct DNA damage) and 320-400 nm (physiological alterations), were occurring when the lights were irradiated in combination (sequentially and simultaneously). The FX-1 310 nm weakened the microorganism due to its increased spectral emission in the 320-400 nm region, making it much more susceptible and easier to damage with the other wavelengths. The order of irradiation in SE mode was found to be crucial to obtain a synergistic effect. Among the synergistic combinations, the irradiation of all three wavelengths, simultaneously, was

**Table 5**  
Device emission characteristics.

UV source	Output efficiency	LED power output (mW)	LED viewing angle	Peak intensity (mW cm <sup>-2</sup> )	UV dose at 2 L min <sup>-1</sup> (mJ cm <sup>-2</sup> )	Peak wavelength (nm)
FX-1 265	2.29 %	70	130°	35.0 ± 5.5	26.7	269.03
FX-1 275	1.32 %	8	150°	51.8 ± 4.4	39.0	277.74
FX-1 310	2.38 %	50	120°	52.8 ± 9.9	39.8	309.51

found to be an energy efficient process when compared to each source acting alone. Further consideration of the emission spectrum by custom selection of light sources could result in potential for faster and more efficient disinfection systems. In conjunction with designing efficient systems, multiple wavelengths on single devices could also assist in reduced electrical energy consumption.

#### 4. Materials and Methods

##### 4.1. Water matrix

A 2-litre water matrix has been used for disinfection experiments in this study. The buffered water matrix (BW) consisted of 0.9% sodium chloride (NaCl) in ultrapure water (MilliQ, 18.2 MΩ cm) previously sterilized at an initial *E. coli* K12 concentration of 10<sup>6</sup> CFU/mL. The second water matrix (WW) used in this study is from the tertiary effluent of the wastewater treatment plant (WWTP) at Rey Juan Carlos University facilities (Mostoles, Spain). 2 L of tertiary effluent has been extracted for each experiment and spiked with *wild E. coli* at an initial concentration of 10<sup>6</sup> CFU/mL.

##### 4.2. Microorganism propagation and enumeration

A culture of *E. coli* K12 (CECT 4624) and *wild E. coli* was added into 20 mL of sterile Luria-Bertan (LB) Broth, separately, and incubated at 37°C for 24h under stirring until a concentration of 10<sup>9</sup> CFU/mL was obtained. 2 mL of the incubated broth solution was then centrifuged at 3500 rpm for 25 min. The cells were washed off the LB broth and resuspended in sterilized 0.9% NaCl solution prior to its use in experiments. *Wild E. coli* culture has been isolated from the tertiary effluent of the WWTP. *Wild E. coli* was isolated from samples from this effluent following the streak plate protocol into MacConkey selective agar plates and incubated for 24 hours under stirring before isolating 4-8 individual colonies of the microorganism. Then, they were grown in LB broth under similar conditions to *E. coli* K12.

For enumeration, irradiated samples were serially diluted in sterilized 0.9% NaCl solution before plating in Miller's LB agar plates, for *E. coli* K12 based experiments, and in Tryptic Soy Agar (TSA) plates, for *wild E. coli* based experiments. For *wild E. coli* experiments, total aerobic bacteria have been tracked and hence TSA plates have been chosen. Drops of 10 μL were spread on agar and incubated inverted at 37°C for 24 h for LB agar, and 48 h for TSA agar for *E. coli* K12 and *wild E. coli* respectively. Samples were plated in triplicates. Plates yielding 10 to 100 colonies were included in the analysis.

##### 4.3. Wastewater quality characterization

Before conducting experiments, it is crucial to evaluate the quality of water being used. All the analyses were repeated a minimum of 3 times per sample and monitored throughout the period of experimentation. In this work, pH was measured using benchtop pH meter (pH 50 VioLab, Dostmann). The pH of wastewater used in this study was found to be 7.5 ± 0.1, meaning that the water is neutral and within the optimal range required for disinfection process.

Conductivity of the input wastewater was measured using a conductometer (712 conductometer, Metrohm). It was measured to be 752 ± 4 μS cm<sup>-1</sup>, which indicates a mid-range conductivity (200 - 1000 μS

cm<sup>-1</sup>) prominent in wastewaters from facilities (Tchobanoglous and Burton, 1990). Transmission of wastewater was measured using a UV-Vis-NIR Spectrophotometer (Cary 5000, Agilent). The transmittance of the wastewater (See Section G, SI), at the peak wavelength, was seen to be 99.37%, 99.95%, and 100%, for FX-1 265, 275, and 310, respectively.

The TOC concentration is a measure of the level of organic molecules or contaminants in water. This is an analytical technique that helps understand whether the water is pure enough for further discharge or, in this case, for further studies. To ensure that the wastewater effluent has a low level of TOC, 20 mL of the effluent was filtered using a 0.20 μm nylon membrane (Millex - GN, Merck Millipore) and placed in TOC-L (TOC analyzer, Shimadzu) for measurement. For the period of time of the experiments in this study, the TOC in the matrix was measured to be 23.3 ± 3.3 mg L<sup>-1</sup>. A constant TOC reading also indicates the presence of a persistent organic contaminant and helps ensure that successive experiments are repeatable and reproducible (Eaton et al., 2005). The TOC level was also monitored before and after irradiation experiments and was seen that the readings were within the instrumental error of the equipment and there was no significant reduction in TOC readings (± 5%).

##### 4.4. UV irradiation

The selection of UV LEDs plays a key role in the rate of disinfection observed. For this study, a wide range of LEDs centered in the ultraviolet (UV) region of the spectrum were considered and studied before their use in experiments. LEDs were selected based on a pre-established selection criterion. The LEDs chosen for this work were 265 nm (KL265-50U-SM-WD, Klaran), 275 nm (XBT-1313-UV-A150-AG270-00, Luminus) and 310 nm (EOLS-310-697, EpiGap). Selected LEDs have been built on to the COBRA Clean FX-1 (earlier called FX-1) from ProPhotonix IRL (ProPhotonix, 2022). The device has been redesigned to fit in UV-C LEDs chosen according to their footprint and has an emitting window size of 76.8 mm × 28 mm. The 265 nm and 310 nm devices accommodated 16 LEDs each (Fig. 3(a, c)), due to the size of the 275 nm LEDs (1.35 mm × 1.35 mm), 64 LEDs were accommodated on the device (Fig. 3(b)). Light emission is controlled by a conditioner driver that uses 48V DC safe current and a 0-10 volts analogue signal corresponding to 0-100 percent intensity range. To measure irradiance in water, ferrioxalate actinometry has been conducted before proceeding with inactivation experiments. Ferrioxalate actinometry was conducted as per the procedure used in Hatchard and Parker, 1956 in recirculation mode as the technique required extended exposure times to calculate the incident irradiation (E s<sup>-1</sup>). Spectral measurements have been made to ensure that the emission of the LEDs is within the scope and interest of this study using ILT spectroradiometer coupled with the RAA4 optic (2003357U1, International Light Technologies) and presented in Fig. 3 (d). The measured emission characteristics of the devices have been listed in Table 5.

##### 4.5. Experimental set-up

To conduct inactivation experiments using multiple combinations, a custom designed UV fixture was manufactured. The designed UV fixture can accommodate up to 8 FX-1's and a quartz tube. The quartz tube can be connected to the sampling tank and outlet to enable a single pass flow

through system (See Fig. 3(e)). The quartz tube used for this study has an external diameter of 23 mm and an inner diameter of 20 mm (FAB028553, Multi-Lab Ltd).

The set-up used is a single pass flow-through system with a pump (at flow rate of 2 L min<sup>-1</sup> and corresponding residence time of 0.75 s) connected to the inlet tank. The active irradiated volume within this setup was 28.27 cm<sup>3</sup>. Three samples have been extracted from the outlet in each experiment. Each combination has been tested a minimum of 4 replicates on separate days to ensure the repeatability and reproducibility of the results. As the system is a single pass system, two radiant intensities (50% and 100%) of the devices have been tested for each combination to evaluate overall UV dose response. The 310 nm individual wavelength irradiation experiments were conducted in recirculation mode until 1-log reduction was observed to evaluate a dependable log reduction per pass as it is known that this wavelength requires longer exposure times for significant log reduction of the model bacterium (Ahmad, 2017).

#### 4.5.1. UV combinations

Multiple combinations of the chosen light sources have been tested. Fig. 3(f-h) represents the different combinations attempted in this study. Individual wavelength mode (IW, Fig. 3(f)) involves the use of only one device on the UV fixture. Sequential mode (SE, Fig. 3(g)) involves the irradiation of 2 wavelengths, at the same time but one after the other, on the water flowing through the system. In this SE mode of irradiation, both possible orders of irradiation of wavelengths have been attempted in each combination (i.e., 265 followed by 310 and vice versa) to evaluate if the order impacted the inactivation rates obtained. In simultaneous mode (SI, Fig. 3(h)), both wavelengths are acting at the same point at an instant of time.

#### 4.6. Residence time and kinetic constants

The kinetic constant ( $k_c$  in s<sup>-1</sup>) for each combination was calculated using Eq. 1 assuming a first-order reaction according to the Chick's law (Bolton and Cotton, 2008; Chick, 1908; Watson, 1908).

$$k_c = - \left( \frac{\text{Log}_{10} \left( \frac{C_0}{C} \right)}{t} \right) \quad (1)$$

where,  $C_0$  is the number of CFU/mL of the unirradiated sample,  $C$  is the CFU/mL for each sample and  $t$  is the residence time in seconds (s). The term  $\text{Log}_{10} (C_0/C)$  is, by definition, the inactivation of bacteria expressed as LRV. It is well known that UV inactivation is fluence-based (Bolton and Linden, 2003). Therefore, the UV dose-response data were fit linearly and the  $\log_{10}$  fluence-based inactivation rate constant,  $k_d$  (cm<sup>2</sup> mJ<sup>-1</sup>) was determined as shown in Eq. 2.

$$k_d = - \left( \frac{\text{Log}_{10} \left( \frac{C_0}{C} \right)}{f_\lambda} \right) \quad (2)$$

where,  $f_\lambda$  is the fluence at the given wavelength,  $\lambda$ , in mJ cm<sup>-2</sup>, determined as shown in Eq. 3.

$$f_\lambda = I \times t \quad (3)$$

being  $I$  the intensity delivered by the light source in mW cm<sup>-2</sup>.

#### 4.7. Synergy of inactivation

The synergy of inactivation has been calculated using Eq. 4 (Koivunen and Heinonen-Tanski, 2005).

$$\text{Synergy} = \frac{k_{\text{combination}}}{k_1 + k_2 + \dots k_n} \quad (4)$$

where,  $k_{\text{combination}}$  is the LRV obtained from actual combination of wavelengths and  $k_{1..n}$  is the LRV obtained from individual wavelength inactivation experiments. Note that the analysis has also been conducted in terms of  $k_c$  (in s<sup>-1</sup>), however all discussions have been presented in terms of LRV.

#### 4.8. Statistical analysis

##### 4.8.1. Student's *t*-distribution analysis

To analyze the statistical significance between the sum of individual inactivation rates and the combined inactivation rates, a *t*-Student distribution analysis was conducted. A one-sided analysis with a confidence level of 95% has been chosen for comparison, as there exists only one factor of comparison between the two datasets under study (Koivunen and Heinonen-Tanski, 2005). The analysis was conducted for each UV source combination tested and compared to the theoretical sum of individual wavelength disinfections obtained. The value of " $t$ " has been retrieved from NIST (NIST, 2023). Data has been collected in triplicates and presented as error bars representing the confidence interval (CI) at 95% confidence level, obtained from *t*-Student analysis. CI was calculated using Eq. 5.

$$CI (95\%) = \pm \frac{t \times SD}{\sqrt{n}} \quad (5)$$

where,  $t$  is the value obtained for  $\nu$  degrees of freedom at 0.05 significant level from the distribution table,  $SD$  is the standard deviation of all the collected samples and  $n$  is the number of samples in the range (Student, 1908). The two datasets under comparison were compared to evaluate if the confidence intervals would overlap meaning that the two intervals are not significantly different and vice versa.

The *t*-test determines if two populations, in this case, theoretical inactivation rates and actual inactivation rates, are statistically different from each other, whereas ANOVA tests can be used to test more than two levels of significance within an independent variable (Simkus, 2022). Hence ANOVA analysis has also been conducted on the data to further establish the validity of data obtained.

##### 4.8.2. Analysis of variance (ANOVA)

ANOVA analyzes categorical independent variables and assumes that the dependent variable follows a normal distribution (Simkus, 2022). In the practical application of this study, the independent variables are considered as categorical since their level can only acquire the on/off values. These levels were codified as -1/+1 (ON/OFF) for each factor (in this case, individual wavelength effect and their combination effect) under investigation. For each lamp arrangement, a full factorial design of experiments was performed to determine the effect of each factor and the interactions thereof (Table S4). The logarithmic reduction value (LRV) and the kinetic constant ( $k_c$ ) were selected as responses. The homogeneity of variances was checked using the Cochran's test and the Student–Newman–Keuls (SNK) test was applied to detect significant differences amongst treatments (Figure S4). The statistical analysis was performed with Statgraphics Centurion XVI (Statgraphics Technologies, Inc. The Plains, Virginia, USA). This technique is based on fitting the data to a surface response corresponding to a balanced two-level full factorial design (Reichardt, 2019), whose model is shown in Eq. 6.

$$Y = a_0 + (a_1 \times x_1) + (a_2 \times x_2) + (a_3 \times x_1 \times x_2) \quad (6)$$

where,  $a_0$  is a coefficient signifying no effect (in this case - dark),  $a_1$  is the coefficient for  $x_1$  effect (265 nm),  $a_2$  is the coefficient for  $x_2$  effect (275 nm) and  $a_3$  is the coefficient for  $x_1 \times x_2$  interaction effect (265 + 275) and  $Y$  is the response,  $k$  or LRV in this case. If the last factor ( $a_3 \times x_1 \times x_2$ )

is statistically significant, it means that the sum of the two  $(a_1 \times x_1) + (a_2 \times x_2)$  factors is not enough to describe the global results of the combination of the two factors. If  $a_3 > 0$ , then the analysis can conclude possible synergistic effect and  $a_3 < 0$  means possible antagonism between the wavelengths under study (Reichardt, 2019). In total, for each combination (and each experimental design), the number of replicates that have been tested has been maintained at 18. Note that for the 3 wavelength combinations, the above analysis has been changed to a three factor-two level full factorial design (Table S4).

#### 4.9. Error propagation

In this study, error analysis plays a vital role in understanding the results and forming evidence-based discussions on the data obtained. For this reason, a detailed error propagation has been conducted (Error Propagation, 2020). In cases involving the calculation of error in sum (for instance Eq. 7), Eq. 8 has been used.

$$(Z \pm \Delta z) = (X \pm \Delta x) + (Y \pm \Delta y) \quad (7)$$

$$\Delta z = \sqrt{(\Delta x)^2 + (\Delta y)^2} \quad (8)$$

In the case of synergy of inactivation (Eq. 4), where the error needs to be calculated in a division (for instance Eq. 9), the error propagation has been done as seen in Eq. 10.

$$(Z \pm \Delta z) = \frac{(X \pm \Delta x)}{(Y \pm \Delta y)} \quad (9)$$

$$\Delta z = Z \times \sqrt{\left(\frac{\Delta x}{X}\right)^2 + \left(\frac{\Delta y}{Y}\right)^2} \quad (10)$$

#### 4.10. Dark control experiments

Dark control experiments were also conducted to ensure the photo-activated nature of the inactivation results and to ensure a robust statistical analysis. To do this, the water matrix was spiked with the microorganism and run through the reactor in the absence of any irradiation. The experiment was conducted a minimum of 4 times and samples were plated in triplicates.

#### 4.11. Electrical energy consumption

Electrical energy per order of inactivation is an important parameter in evaluating the efficiency of a disinfection process (Keen et al., 2018). It is defined as the energy required to reduce the microbial population by one order of magnitude (i.e., ten-fold reduction, LRV = 1.0). To compare the electrical efficiency of each wavelength with possible combination of wavelengths, the electrical energy per order ( $E_{EO}$ , kWh m<sup>-3</sup>) has been calculated according to Eq. 11 (Keen et al., 2018).

$$E_{EO} = \frac{P}{Q \times \log_{10} \left( \frac{C_0}{C} \right)} \quad (12)$$

where,  $P$  is the electrical energy consumed in each process (the sum of energy consumed by pump and lamps) in kW,  $Q$  is the inlet flow rate in m<sup>3</sup> h<sup>-1</sup>, and  $\log_{10} (C_0/C)$  is the LRV (Keen et al., 2018).

#### CRediT authorship contribution statement

**Adithya Pai Uppinakudru:** Investigation, Methodology, Data curation, Writing – original draft. **Miguel Martín-Sómer:** Validation, Supervision, Writing – review & editing. **Ken Reynolds:** Conceptualization, Supervision, Resources, Writing – review & editing. **Simon Stanley:** Supervision, Validation, Resources, Writing – review & editing. **Luis Fernando Bautista:** Data curation, Resources, Supervision,

Writing – review & editing. **Cristina Pablos:** Validation, Supervision, Writing – review & editing. **Javier Marugán:** Funding acquisition, Validation, Supervision, Writing – review & editing.

#### Declaration of competing interest

The authors declare that they have no known competing financial interests or personal relationships that could have appeared to influence the work reported in this paper.

#### Data availability

Data will be made available on request.

#### Acknowledgements

The authors acknowledge the financial support of the European Union's Horizon 2020 research and innovation programme in the frame of REWATERGY, Sustainable Reactor Engineering for Applications on the Water-Energy Nexus, MSCA-ITN-EID Project N. 812574. We thank Cristina Ramírez-Miguel and María Luisa Perez-Araújo for technical assistance.

#### Supplementary materials

Supplementary material associated with this article can be found, in the online version, at doi:10.1016/j.wroa.2023.100208.

#### References

- Ahmad, S.I., 2017. Reactive oxygen species in biology and human health. CRC Press. <https://doi.org/10.1201/b20228>.
- Ashok, A., Khedikar, P.I.P., 2016. Overview of water disinfection by UV technology -A review. Water Research. <https://doi.org/10.13140/RG.2.2.30976.25608>.
- Beck, S.E., Ryu, H., Boczek, L.A., Cashdollar, J.L., Jeanis, K.M., Rosenblum, J.S., Lawal, O.R., Linden, K.G., 2017. Evaluating UV-C LED disinfection performance and investigating potential dual-wavelength synergy. Water Research 109, 207–216. <https://doi.org/10.1016/j.watres.2016.11.024>.
- Bolton, J.R., Cotton, C.A., 2008. Ultraviolet (UV) disinfection for Water Treatment, second edition. Awwa. URL: <https://engage.awwa.org/PersonifyEbusiness/Bookstore/Product-Details/productId/92298805>.
- Bolton, J.R., Linden, K.G., 2003. Standardization of methods for fluence (UV dose) determination in bench-scale UV experiments. Journal of Environmental Engineering (New York, N.Y.) 129 (3), 209–215. [https://doi.org/10.1061/\(asce\)0733-9372\(2003\)129:3\(209\)](https://doi.org/10.1061/(asce)0733-9372(2003)129:3(209)).
- Chick, H., 1908. An investigation of the laws of disinfection. The Journal of Hygiene (8-1), 92–158. <https://doi.org/10.1017/s0022172400006987>.
- COBRA Clean FX-1, 2022. ProPhotonix IRL. URL <https://www.prophotonix.com/led-and-laser-products/uv-c-led-systems/uv-c-led-system/> (Accessed 10/12/2022).
- Cockell, C.S., Airo, A., 2002. Origins of Life and Evolution of the Biosphere: The Journal of the International Society for the Study of the Origin of Life 32 (3), 255–274. <https://doi.org/10.1023/a:1016507810083>.
- Collivignarelli, M.C., Abbà, A., Miino, M.C., Caccamo, F.M., Torretta, V., Rada, E.C., Sorlini, S., 2021. Disinfection of Wastewater by UV-Based Treatment for Reuse in a Circular Economy Perspective. Where Are We at? International Journal of Environmental Research and Public Health 18 (1), 77. <https://doi.org/10.3390/ijerph18010077>.
- Eaton, A. D., Franson, M. A. H., 2005. Standard methods for the examination of water & wastewater. Centennial ed. /Washington. American Public Health Association. 21. URL <https://engage.awwa.org/PersonifyEbusiness/Bookstore/Product-Details/productId/162167531>.
- Eisenstark, A., Calcutt, M.J., Becker-Hapak, M., Ivanova, A., 1996. Role of Escherichia coli rpoS and associated genes in defense against oxidative damage. Free Radical Biology & Medicine (21-7), 975–993. [https://doi.org/10.1016/s0891-5849\(96\)00154-2](https://doi.org/10.1016/s0891-5849(96)00154-2).
- Error Propagation., 2020. Uncertainty Analysis for Engineers and Scientists, 181–232. <https://doi.org/10.1017/978110877513.006>.
- Green, A., Popović, V., Pierscianowski, J., Biancaniello, M., Warriner, K., Koutchma, T., 2018. Inactivation of Escherichia coli, Listeria and Salmonella by single and multiple wavelength ultraviolet-light emitting diodes. Innovative Food Science & Emerging Technologies: IFSET: The Official Scientific Journal of the European Federation of Food Science and Technology. 47, 353–361. <https://doi.org/10.1016/j.ifset.2018.03.019>.
- Hatchard, C. G., Parker, C. A., 1956. A new sensitive chemical actinometer - II. Potassium ferrioxalate as a standard chemical actinometer. Proceedings of the Royal Society of London. 235-1203, 518–536. <https://doi.org/10.1098/rspa.1956.0102>.

- Hiraku, Y., Ito, K., Hirakawa, K., Kawanishi, S., 2007. Photosensitized DNA damage and its protection via a novel mechanism. *Photochemistry and Photobiology* 205–212. <https://doi.org/10.1562/2006-03-09-IR-840>, 83-1.
- Hull, N.M., Linden, K.G., 2018. Synergy of MS2 disinfection by sequential exposure to tailored UV wavelengths. *Water Research* 143, 292–300. <https://doi.org/10.1016/j.watres.2018.06.017>.
- Kang, J.-W., Kang, D.-H., 2019. The synergistic bactericidal mechanism of simultaneous treatment with a 222-nanometer krypton-chlorine excilamp and a 254-nanometer low-pressure mercury lamp. *Applied and Environmental Microbiology* 85–91. <https://doi.org/10.1128/AEM.01952-18>.
- Keen, O., Bolton, J., Litter, M., Bircher, K., Oppenländer, T., 2018. Standard reporting of Electrical Energy per Order (EEO) for UV/H<sub>2</sub>O<sub>2</sub> reactors (IUPAC Technical Report). *Pure and Applied Chemistry* 1487–1499. <https://doi.org/10.1515/pac-2017-0603>, 90-9.
- Koivunen, J., Heinonen-Tanski, H., 2005. Inactivation of enteric microorganisms with chemical disinfectants, UV irradiation and combined chemical/UV treatments. *Water Research* 1519–1526. <https://doi.org/10.1016/j.watres.2005.01.021>, 39-8.
- Kuball, H.-G., Höfer, T., Kiesewalter, S., 2017. Chiroptical Spectroscopy. *General Theory*. *Encyclopaedia of Spectroscopy and Spectrometry*. Elsevier, pp. 217–231. <https://doi.org/10.1016/B978-0-12-409547-2.04980-5>.
- Kumar, A., Ghate, V., Kim, M.-J., Zhou, W., Khoo, G.H., Yuk, H.-G., 2015. Kinetics of bacterial inactivation by 405nm and 520nm light emitting diodes and the role of endogenous coproporphyrin on bacterial susceptibility. *Journal of Photochemistry and Photobiology. B, Biology*. 149, 37–44. <https://doi.org/10.1016/j.jphotobiol.2015.05.005>.
- Li, G.-Q., Wang, W.-L., Huo, Z.-Y., Lu, Y., Hu, H.-Y., 2017. Comparison of UV-LED and low pressure UV for water disinfection: Photoreactivation and dark repair of *Escherichia coli*. *Water Research* 126, 134–143. <https://doi.org/10.1016/j.watres.2017.09.030>.
- Maclean, M., MacGregor, S.J., Anderson, J.G., Woolsey, G., 2008. High-intensity narrow-spectrum light inactivation and wavelength sensitivity of *Staphylococcus aureus*. *FEMS Microbiology Letters* 227–232. <https://doi.org/10.1111/j.1574-6968.2008.01233.x>, 285-2.
- Martín-Sómer, M., Pablos, C., Adán, C., van Grieken, R., Marugán, J., 2023. A review on LED technology in water photodisinfection. *Science of the Total Environment*, 163963. <https://doi.org/10.1016/j.scitotenv.2023.163693>, 885-10.
- Matafonova, G., Batoev, V., 2022. Dual-wavelength light radiation for synergistic water disinfection. *Science of the Total Environment*. <https://doi.org/10.1016/j.scitotenv.2021.151233>, 806-3, 151233.
- Mecha, A.C., Onyango, M.S., Ochieng, A., Momba, M.N.B., 2017. Evaluation of synergy and bacterial regrowth in photocatalytic ozonation disinfection of municipal wastewater. *The Science of the Total Environment* 626–635. <https://doi.org/10.1016/j.scitotenv.2017.05.204>, 601–602.
- Nakahashi, M., Mawatari, K., Hirata, A., Maetani, M., Shimohata, T., Uebanso, T., Hamada, Y., Akutagawa, M., Kinouchi, Y., Takahashi, A., 2014. Simultaneous irradiation with different wavelengths of ultraviolet light has synergistic bactericidal effect on *Vibrio parahaemolyticus*. *Photochemistry and photobiology* 1397–1403. <https://doi.org/10.1111/php.12309>, 90-6.
- NIST., 2023. Critical Values of the Student's t Distribution. *Engineering Statistics Handbook*. URL <https://www.itl.nist.gov/div898/handbook/eda/section3/eda3672.htm> (Accessed 06/04/23).
- Nyangaresi, P.O., Qin, Y., Chen, G., Zhang, B., Lu, Y., Shen, L., 2019. Comparison of the performance of pulsed and continuous UVC-LED irradiation in the inactivation of bacteria. *Water Research* 157, 218–227. <https://doi.org/10.1016/j.watres.2019.03.080>.
- Oguma, K., Kita, R., Sakai, H., Murakami, M., Takizawa, S., 2013. Application of UV light emitting diodes to batch and flow-through water disinfection systems. *Desalination* 328, 24–30. <https://doi.org/10.1016/j.desal.2013.08.014>.
- Payne, G., Sancar, A., 1990. Absolute action spectrum of E-FADH<sub>2</sub> and E-FADH<sub>2</sub>-MTHF forms of *Escherichia coli* DNA photolyase. *Biochemistry* 7715–7727. <https://doi.org/10.1021/bi00485a021>, 29-33.
- Pizarro, R.A., 1995. UV-A oxidative damage modified by environmental conditions in *Escherichia coli*. *Int J Radiat Biol* 68 (3), 293–299. <https://doi.org/10.1080/09553009514551221>.
- Rastogi, R.P., Richa Kumar, A., Tyagi, M.B., Sinha, R.P., 2010. Molecular mechanisms of ultraviolet radiation-induced DNA damage and repair. *Journal of Nucleic Acids* 2010, 592980. <https://doi.org/10.4061/2010/592980>.
- Regulation (EU) 2020/741, 2022. Commission Notice Guidelines to support the application of Regulation 2020/741 on minimum requirements for water reuse 2022/C 298/01. Web Article. URL <https://shorturl.at/hFGO4>.
- Reichardt, C.S., 2019. Quasi-experimentation: A guide to design and analysis. Guilford Publications. URL <https://www.guilford.com/books/Quasi-Experimentation/Charles-Reichardt/9781462540204>.
- Rodríguez-Chueca, J., García-Cañibano, C., Sarro, M., Encinas, Á., Medana, C., Fabbri, D., Calza, P., Marugán, J., 2019. Evaluation of transformation products from chemical oxidation of micropollutants in wastewater by photoassisted generation of sulfate radicals. *Chemosphere* 226, 509–519. <https://doi.org/10.1016/j.chemosphere.2019.03.152>.
- Rout, P.R., Zhang, T.C., Bhunia, P., Surampalli, R.Y., 2021. Treatment technologies for emerging contaminants in wastewater treatment plants: A review. *The Science of the total environment* 753, 141990. <https://doi.org/10.1016/j.scitotenv.2020.141990>.
- Simkus, J., 2022. *What is ANOVA (Analysis Of Variance)*. Simply Psychology. Web Article. URL [www.simplypsychology.org/anova.html](http://www.simplypsychology.org/anova.html) (Accessed 23/03/23).
- Song, K., Mohseni, M., Taghipour, F., 2016. Application of ultraviolet light-emitting diodes (UV-LEDs) for water disinfection: A review. *Water Research* 94, 341–349. <https://doi.org/10.1016/j.watres.2016.03.003>.
- Student., 1908. The Probable Error of a Mean. *Biometrika*, 1. <https://doi.org/10.2307/2331554>, 6-1.
- Tang, W.Z., Sillanpää, M., 2015. Bacteria sensitivity index of UV disinfection of bacteria with shoulder effect. *Journal of Environmental Chemical Engineering* (3-4), 2588–2596. <https://doi.org/10.1016/j.jece.2015.09.010>.
- Tchobanoglous, G., Burton, F., 1990. *Wastewater engineering: Treatment, Disposal, Reuse*. McGraw-Hill Inc., USURL <https://www.iberlibro.com/9780070416901/Wastewater-Engineering-Treatment-Disposal-Reuse-0070416907/plp> (Accessed 18/04/23).
- WASH in health care facilities: Global baseline report 2019. 2019. UNICEF. URL <https://data.unicef.org/resources/wash-in-health-care-facilities/> (Accessed 12/04/23).
- Wastewater Contaminants Research, 2023. United States Environmental Protection Agency. URL <https://www.epa.gov/water-research/wastewater-contaminants-research> (Accessed 18/04/2023).
- Water Quality and Wastewater. 2023. UN Water. URL <https://www.unwater.org/water-facts/water-quality-and-wastewater> (Accessed 12/04/23).
- Watson, H.E., 1908. A note on the variation of the rate of disinfection with change in the concentration of the disinfectant. *The Journal of Hygiene* (8-4), 536–542. <https://doi.org/10.1017/s0022172400015928>.
- Woo, H., Beck, S.E., Boczek, L.A., Carlson, K., Brinkman, N.E., Linden, K.G., Lawal, O.R., Hayes, S.L., Ryu, H., 2019. Efficacy of inactivation of human enteroviruses by dual-wavelength germicidal ultraviolet (UV-C) light emitting diodes (LEDs). *Water* 1–1131. <https://doi.org/10.3390/w11061131>, 11-6.